An Automatic Frequency Control Loop Using Overlapping DFTs

S. Aguirre
Communications Systems Research Section

An automatic frequency control (AFC) loop is introduced and analyzed in detail. The new scheme is a generalization of the well-known Cross-Product AFC loop that uses running overlapping discrete Fourier transforms (DFTs) to create a discriminator curve. Linear analysis is included and supported with computer simulations. The algorithm is tested in a low carrier to noise ratio (CNR) dynamic environment, and the probability of loss of lock is estimated via computer simulations. The algorithm discussed is a suboptimum tracking scheme with a larger frequency error variance compared to an optimum strategy, but offers simplicity of implementation and a very low operating threshold CNR. This technique can be applied during the carrier acquisition and re-acquisition process in the Advanced Receiver.

I. Introduction

Automatic frequency tracking is a subject of great importance in the fields of communications, control, and signal processing. For instance, it may provide initial rapid acquisition in coherent receivers, may supply information on the velocity of rapidly moving targets, and can be used in conjunction with channel doppler extractors, just to name a few applications.

This article presents a study of the fundamental problem of estimating the frequency of a sinusoidal wave embedded in noise, subject to severe dynamics. It is well known [1], [2] that the maximum likelihood estimator (MLE) of a constant (but unknown) frequency sine wave is equivalent in practice to a discrete Fourier transform (DFT) operation on the received discrete data, the MLE of frequency being the center frequency of the bin filter in the DFT with maximum output power. For a stable frequency, arbitrarily good resolution is obtained by increasing the size of the DFT or, equivalently, by extending the observation interval. However, when the frequency of the incoming wave is time varying in a random manner, the implementation of a maximum likelihood approach may be computationally demanding, as discussed in [3], [4].

The object of this article is to propose and analyze a suboptimum frequency control loop based on short overlapping DFTs and suited to track the rapidly varying frequency of a sine wave. For brevity, the new scheme will be referred to here as ODAFC (Overlapping Discrete Fourier transform-based Automatic Frequency Control). This scheme can be thought of as a generalization of the so-called Quadri-Correlator [5]. The new scheme integrates ideas originating in the fields of classical spectral estimation and digital phase-locked loop theory. It will be shown that the ODAFC is capable of track-

ing the frequency of a carrier signal in a low carrier-to-noise (CNR) and high dynamic environment where a Phase-Locked Loop (PLL) is inoperative. Such a situation is foreseeable during planetary encounters. In these cases ODAFC will allow fast carrier re-acquisition and help the resumption of tracking itself. This is achieved with remarkably modest implementation complexity, since the algorithm may be implemented in software and does not require any modification to the Advanced Receiver (ARX) hardware.

First, as an indicator of the quality of the closed loop estimator, the variance of the loop is computed for a fixed frequency sine wave in the presence of additive white Gaussian noise (AWGN). Later, the loop is tested with severe dynamics and noise together, and the probability of loss of lock is estimated. Both analytical answers (whenever possible) and computer simulation results are included for greater confidence.

II. Description of the ODAFC Loop

A. System Block Diagram

A block diagram of the ODAFC loop is shown in Fig. 1(a). An equivalent baseband model is shown in Fig. 1(b). The discrete time in-phase and quadrature mixer outputs admit a representation of the form

$$I_n = A\cos(\phi_n) + n_{In} \tag{1a}$$

$$Q_n = A\sin(\phi_n) + n_{Qn} \tag{1b}$$

The amplitude A is related to the carrier power via $A^2 = P_c$, the instantaneous phase error is given by ϕ_n (rad), and the noise sequences $\{n_{In}\}$, $\{n_{Qn}\}$ are independent Gaussian random variables with zero mean and variance $\sigma^2 = N_o/2T_s$, where T_s is the loop update time (henceforth called the sampling interval). The carrier-to-noise ratio is defined as CNR = P_c/N_o. Every update time, N_s complex samples are Fourier transformed with N_s zeroes appended. At the tick of the clock, the data are shifted when another complex sample arrives; a new discrete Fourier transform is computed (of size $2N_s$), an error control signal is created and the loop filter is updated. This process is repeated every sampling interval T_s, each time incorporating just one more complex sample. A timing diagram of the underlying process is illustrated in Fig. 2.

B. On the Discriminator Characteristic

It is well known that the discrete Fourier transform can be seen as a bank of bandpass filters tuned at multiples of half the Nyquist rate [6]. In order to create a control signal proportional to the frequency error (discriminator characteristic), the powers in two adjacent filter bins around zero frequency are subtracted every sampling interval (a weighted combination of the filter bin outputs was not selected to facilitate the implementation). The subtraction of the powers in the bin filters around zero frequency to create a discriminator curve as opposed to selecting the bin filter with maximum power was originally discussed in [7]. The idea of employing running overlapping DFTs has a connection with the use of the FFT for the estimation of power spectra based on averaged periodograms [8].

III. Linear Tracking of the ODAFC Loop in the Presence of Noise

A. Exact Computation of the Variance of the Frequency Error

This section focuses on the tracking performance of the ODAFC loop when the carrier-to-noise ratio is sufficiently high to justify a linear analysis. A sine wave with constant frequency is assumed for the remainder of the section. The goal is to compute analytically an expression that predicts the variance of the closed loop estimator. The results will be confirmed by computer simulations.

The closed loop estimator uses the received complex sample

$$x_n = I_n + jQ_n \tag{2}$$

and computes

$$X_{k,\ell} = \frac{1}{N_s}\sum_{n=k-(N_s-1)}^{k} x_n e^{-j2\pi\ell n/2N_s} \triangleq R_{k,\ell} + jM_{k,\ell} \tag{3}$$

The discriminator output at time $n = k$ is given by

$$P_k = R_{k,1}^2 + M_{k,1}^2 - (R_{k,-1}^2 + M_{k,-1}^2)$$

$$= \left(\frac{1}{N_s}\right)^2 \sum_{m=k-(N_s-1)}^{k}\sum_{n=k-(N_s-1)}^{k} 2(I_nQ_m - Q_nI_m) \times \sin\left(\frac{\pi}{N_s}(m-n)\right) \tag{4}$$

which upon expansion results in

$$P_k \triangleq S_k + N_{\text{eq},k} \tag{5}$$

where

$$S_k = 2\left(\frac{1}{N_s}\right)^2 \sum_{m=k-(N_s-1)}^{k} \sum_{n=k-(N_s-1)}^{k} A^2 \sin(\phi_m - \phi_n) \times \sin\left(\frac{\pi}{N_s}(m-n)\right) \tag{6}$$

$$N_{\mathrm{eq},k} = 2\left(\frac{1}{N_s}\right)^2 \sum_{m=k-(N_s-1)}^{k} \sum_{n=k-(N_s-1)}^{k} \{A\, n_{Qm}\cos(\phi_n) + A\, n_{In}\sin(\phi_m) - A\, n_{Im}\sin(\phi_n) - A\, n_{Qn}\cos(\phi_m) + n_{In}\, n_{Qm} - n_{Qn}\, n_{Im}\} \times \sin\left(\frac{\pi}{N_s}(m-n)\right) \tag{7}$$

for a fixed frequency error; $S_k(\cdot)$ denotes the discriminator characteristic for the ODAFC loop, and it is given more explicitly in Eq. (8).

$$S_k(\Delta\omega_k T_s) = A^2\left\{\left[\frac{\sin\left(\frac{\Delta\omega_k N_s T_s}{2} - \frac{\pi}{2}\right)}{\sin\left(\frac{\Delta\omega_k T_s}{2} - \frac{\pi}{2N_s}\right)}\right]^2 - \left[\frac{\sin\left(\frac{\Delta\omega_k N_s T_s}{2} + \frac{\pi}{2}\right)}{\sin\left(\frac{\Delta\omega_k T_s}{2} + \frac{\pi}{2N_s}\right)}\right]^2\right\} \tag{8}$$

The slope at the origin is

$$S_k'(\Delta\omega_k T_s)\Big|_{\Delta\omega_k T_s = 0} = A^2\left(\frac{1}{N_s}\right)^2\left\{\frac{8\pi^2\cos\left(\frac{\pi}{2N_s}\right)}{\sin^3\left(\frac{\pi}{2N_s}\right)}\right\} \tag{9}$$

The discriminator characteristic is illustrated in Fig. 3 for a unit amplitude signal ($A = 1$) for $N_s = 2,4$ corresponding to DFTs of sizes 4 and 8, respectively; notice that a larger slope for the discriminator at the origin is obtained with larger DFTs. For a fixed frequency sine wave in the presence of AWGN, the larger the size of the DFT, the smaller the variance of the estimator. However, in a dynamic medium, the maximum permissible size for the DFT is limited by how fast the center frequency is moving, since larger DFTs have a smaller linear operating range.

The term $N_{\mathrm{eq},k}$ will be referred to as the additive equivalent noise. Unfortunately, the typical white noise assumption for the equivalent noise is not justified here, since there exists a significant amount of correlation between the noise samples. It is shown in Appendix A that the correlation function of the noise sequence $\{N_{\mathrm{eq},k}\}$ is given by

$$R_{N_{\mathrm{eq}}}(\ell) = \mathbb{E}(N_{\mathrm{eq},k}\, N_{\mathrm{eq},k+\ell}) = 8\left(\frac{1}{N_s}\right)^4 A^2\sigma^2\frac{(N_s - |\ell|)\cos\left(\frac{\pi\ell}{N_s}\right)}{\left[\sin\left(\frac{\pi}{2N_s}\right)\right]^2} - 8\left(\frac{1}{N_s}\right)^4 A^2\sigma^2\frac{\sin\left(\frac{\pi|\ell|}{N_s}\right)}{\left[\sin\left(\frac{\pi}{2N_s}\right)\right]^2\sin\left(\frac{\pi}{N_s}\right)} + 8\left(\frac{1}{N_s}\right)^4\sigma^4(N_s - |\ell|)^2 - 8\left(\frac{1}{N_s}\right)^4\sigma^4\left[\frac{\sin\left(\frac{\pi\ell}{N_s}\right)}{\sin\left(\frac{\pi}{N_s}\right)}\right]^2 \quad 0 \leqslant |\ell| \leqslant N_s \tag{10}$$

otherwise

$$R_{N_{\mathrm{eq}}}(\ell) = 0$$

With the aid of Fig. 1, it is a straightforward exercise to show that in operational notation the Z transform of the normalized radian frequency error is given by

$$\Delta\Omega(z)\, T_s = H(z)\,\Omega(z)\, T_s - \frac{H(z)}{S_k'(0)} N_{\mathrm{eq}}(z) \tag{11}$$

where

$$H(z) \triangleq \frac{S_k'(0)\,F_2(z)\,NCO(z)\,k_N}{1 + S_k'(0)\,F_2(z)\,NCO(z)\,k_N} \tag{12}$$

represents the closed loop transfer function. The loop filter $F(z)$ considered here has the form

$$F_1(z) = \frac{F_2(z)}{1 - z^{-1}}$$

$$= \left[\frac{k_1}{1 - z^{-1}} + \frac{k_2}{(1 - z^{-1})^2}\right] \frac{1}{S_k'(0)\,k_N\,T_s} \tag{13}$$

where

$$k_1 = \frac{r(4\,B_A\,T_s)}{r + 1}$$

$$k_2 = \frac{k_1^2}{r}$$

$$r = 4\,\xi^2$$

ξ = damping ratio

B_A = nominal bandwidth (Hz)

and $NCO(z)$ is the mathematical model of the numerically controlled oscillator and may include computational delays inherent in a digital implementation. Of particular interest is the *NCO* discussed in [9], which conceptually represents the cascading of an integrator using the trapezoidal rule and two extra delays.

$$NCO(z) = \frac{T_s(z + 1)}{2\,z^2(z - 1)} \tag{14}$$

Since the noise sequence $\{N_{eq,k}\}$ is stationary, the steady state variance of the frequency error (Hz) is given by [10], [11] as

$$\sigma_{\Delta f}^2 = \frac{1}{[S_k'(0)]^2}\left(\frac{1}{2\pi T_s}\right)^2 \frac{1}{2\pi}\int_{-\pi}^{\pi} |H(e^{j\omega})|^2\, S_{N_{eq}}(e^{j\omega})\, d\omega \tag{15}$$

where the equivalent noise spectral density has the form

$$S_{N_{eq}}(e^{j\omega}) = R_{N_{eq}}(0) + 2\sum_{\ell=1}^{N_s-1} R_{N_{eq}}(\ell)\cos(\ell\omega) \tag{16}$$

Unfortunately, the previous integral does not reduce to a simple compact expression as in a standard phase-locked loop [5], and a numerical integration must be used. For illustration purposes, Fig. 4 shows numerical results, based on Eq. (15), for $N_s = 4$ and for a particular mechanization using $T_s = 2 \times 10^{-3}$ s with nominal bandwidth B_A (Hz) as a parameter. Computer simulation results are also included in the same graph to confirm the analysis. Notice that for high CNR, the analysis and the simulations are in excellent agreement.

B. A Useful Approximation for the Variance of the Frequency Error

A very useful approximation to the variance of the frequency error can be obtained for low to moderate CNR when the bandwidth of the loop is much smaller than the sampling rate. The approximation is obtained by expanding the cosinusoidal terms of the noise spectral density of Eq. (16) in a Taylor series and keeping only the significant terms of the expansion. The result is

$$\sigma_{\Delta f}^2 \approx \left(\frac{2}{N_s}\right)^2\left(\frac{1}{2\pi}\right)^3\left(\frac{1}{T_s}\right)^2\left[a\,\Omega_L\,T_s - \frac{b}{3}(\Omega_L\,T_s)^3\right] \tag{17}$$

where

$$a = R_{N_{eq}}(0) + 2\sum_{\ell=1}^{N_s-1} R_{N_{eq}}(\ell) \tag{18}$$

$$b = \sum_{\ell=1}^{N_s-1} \ell^2\, R_{N_{eq}}(\ell) \tag{19}$$

$\Omega_L = 2\pi\,(2B_L)$

B_L = one-sided loop noise bandwidth

The approximation is very tight for small bandwidths ($B_L \lesssim 10$ Hz) and for low CNRs ($\lesssim 30$ dB-Hz), and it loosens as these two parameters increase, until it becomes useless for CNR $\gtrsim 50$ dB-Hz, as shown in Fig. 4.

IV. Steady State Frequency Errors

The steady state frequency error due to acceleration in frequency can be calculated from Eq. (11) in the absence of noise using the final value theorem [12]. The input frequency in the Z domain is given by

$$\Omega(z) = z\left\{\frac{1}{2}J_o t^2\right\}$$

and the steady state error is

$$\Delta f_{ss}(\text{Hz}) = \lim_{z \to 1} \left(\frac{z-1}{z} \right) H(z)\, \Omega(z)$$

$$= \frac{J_o (r+1)^2}{16 B_A^2 r} \cdot \frac{1}{2\pi}$$

where the units of the jerk J_o are in rad/s^3.

V. The ODAFC Loop in a Dynamic Environment

One of the main reasons for this study was the need to operate the frequency estimator under severe dynamic conditions at low CNR levels. It is natural to select the probability of loss of frequency lock as a measure of quality. Once cast into this form, computer simulations provide the most direct way to evaluate performance.

A. Dynamic Trajectory

A dynamic trajectory of duration 8 s was developed to evaluate loop performance. Initially, it is assumed that the phase, frequency, and frequency rate of the received signal are perfectly known, i.e., that the loop is in the tracking mode of operation. The transmitting vehicle then experiences a sudden maneuver resulting in an acceleration of 3 s duration and equivalent to a doppler rate of −1287 Hz/s. For the next 0.5 s, a frequency acceleration of 5150 Hz/s^2 occurs, followed by a 2 s duration doppler rate of 1287 Hz/s. A frequency acceleration of −5150 Hz/s^2 proceeds for the next 0.5 s, and the maneuver culminates with a 2-s-duration doppler rate of −1287 Hz/s.

B. Probability of Loss of Lock for the ODAFC Loop

The probability of losing frequency lock was estimated for a loop that is initially in-lock and then experiences the phase trajectory previously described. The simulations were carried out for various sizes of DFTs, but $N_s = 4$ was found to have the lowest possible threshold with this technique. Some simulation results are presented in Figs. 5 and 6 for $N_s = 4$ and 8, respectively, as a function of carrier to noise ratio (dB-Hz) with nominal loop bandwidth as a parameter. For a given CNR and nominal bandwidth, 250 different simulation runs were employed. Loss of lock was declared when the instantaneous frequency error exceeded the one-sided Nyquist bandwidth $1/2T_s$.

In order to put these results in proper perspective, from [4] a type-3 digital phase-locked loop (DPLL) with the same phase trajectory and an optimized bandwidth, has a probability of 0.1 of losing lock at approximately 26 dB-Hz; i.e., the threshold for a DPLL is about 3 dB higher than that of the ODAFC with $N_s = 4$. From the same reference, the threshold of a typical Cross-Product AFC loop is 2.3 dB-Hz higher than that of the ODAFC.

Estimation of the probability of loss of lock is only a partial performance measure. If in-lock, a phase-locked loop has typically a better frequency estimation ability than the ODAFC loop. In Figs. 7 and 8, the rms value for the ODAFC loop is estimated for the aforementioned trajectory. Notice that when $N_s = 8$, smaller tracking errors are achieved, but the threshold is higher. The same effect is noticed for larger values of N_s. This scheme then suffers from the usual trade-off between noise suppression and dynamic tracking: the effect of the noise increases as N_s decreases, while smaller dynamic errors are obtained as N_s decreases.

VI. Conclusions

A new automatic frequency control loop was introduced and discussed. The algorithm (ODAFC) is based on running overlapping DFTs, and can be viewed as a generalization of the well-known Cross-Product AFC (CPAFC) loop [7]. In fact, the CPAFC is a special case of the ODAFC loop when $N_s = 2$.

A detailed noise analysis was presented of the new algorithm for any desired DFT size, and the analysis supported with computer simulations. In addition, the algorithm was tested in a noisy dynamic medium, and the probability was estimated of loss of lock for various configurations for a specific phase trajectory. It was shown in the text that for this particular trajectory, a value $N_s = 4$ minimizes the operating threshold for this algorithm. In fact, the ODAFC with $N_s = 4$ has a threshold 3 dB-Hz lower than that of a DPLL and comparable to that of a maximum likelihood estimator [4], but with a larger error variance. The implementation complexity for the ODAFC is substantially simpler than for an optimum strategy, not even requiring fast Fourier transforms to compute the DFT when N_s is small.

In summary, the algorithm discussed in this article is a suboptimum tracking scheme with increased variance for the frequency error compared to an optimum strategy, but offers simplicity of implementation and a very low threshold.

Acknowledgments

The author wishes to thank Joseph I. Statman for providing both the dynamic trajectory used to test the loop and for helpful comments. Useful discussions with Sami Hinedi and Vic Vilnrotter are also appreciated.

References

[1] S. L. Marple, Jr., *Digital Spectral Analysis with Applications*, Englewood Cliffs, New Jersey: Prentice-Hall, 1987.

[2] M. S. Kay, *Modern Spectral Estimation*, Englewood Cliffs, New Jersey: Prentice-Hall, 1988.

[3] W. J. Hurd, J. I. Statman, and V. A. Vilnrotter, "High Dynamic GPS Receiver Using Maximum Likelihood Estimation and Frequency Tracking," *IEEE Trans. on Aerosp. and Electr. Syst.*, vol. AES-23, no. 4, pp. 425–437, July 1987.

[4] V. A. Vilnrotter, S. Hinedi, and R. Kumar, *A Comparison of Frequency Estimation Techniques for High Dynamic Trajectories*, JPL Publication 88-21, to be published.

[5] F. M. Gardner, *Phase Lock Techniques*, 2nd ed., New York: John Wiley and Sons, 1979.

[6] G. D. Bergland, "A Guided Tour of the Fast Fourier Transform," *IEEE Spectrum*, vol. 6, pp. 41–52, July 1969.

[7] F. D. Natali, "AFC Tracking Algorithms," *IEEE Trans. on Commun.*, vol. COM-32, no. 8, pp. 935–947, August 1984.

[8] P. D. Welch, "The Use of the Fast Fourier Transform for the Estimation of Power Spectra: A Method Based on Time Averaging Over Short, Modified Periodograms," *IEEE Trans. Audio Electroacoust.*, vol. AU-15, pp. 70–73, June 1967.

[9] S. Aguirre, W. J. Hurd, R. Kumar, and J. I. Statman, "A Comparison of Methods for DPLL Loop Filter Design," *TDA Progress Report 42-87*, vol. July–September 1986, Jet Propulsion Laboratory, Pasadena, California, pp. 114–124, November 15, 1986.

[10] A. V. Oppenheim and R. W. Schafer, *Digital Signal Processing*, Englewood Cliffs, New Jersey: Prentice-Hall, 1975.

[11] W. C. Lindsey and C. M. Chie, "A Survey of Digital Phase-Locked Loops," *Proceedings of the IEEE*, vol. 69, no. 4, pp. 410–430, April 1981.

[12] C. L. Phillips and H. T. Nagle, Jr., *Digital Control System Analysis and Design*, Englewood Cliffs, New Jersey: Prentice-Hall, 1984.

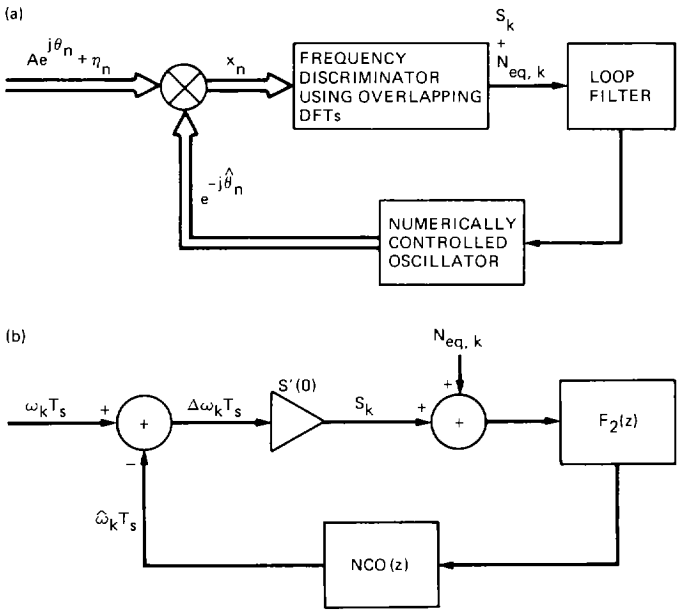

Fig. 1. Two loops: (a) an automatic frequency control loop using overlapping DFTs and (b) an equivalent linearized baseband model

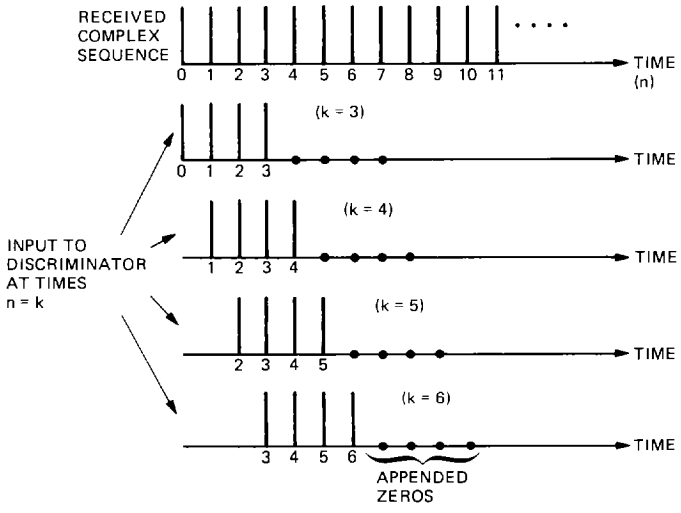

Fig. 2. Overlapping of the received signals to create a discriminator characteristic

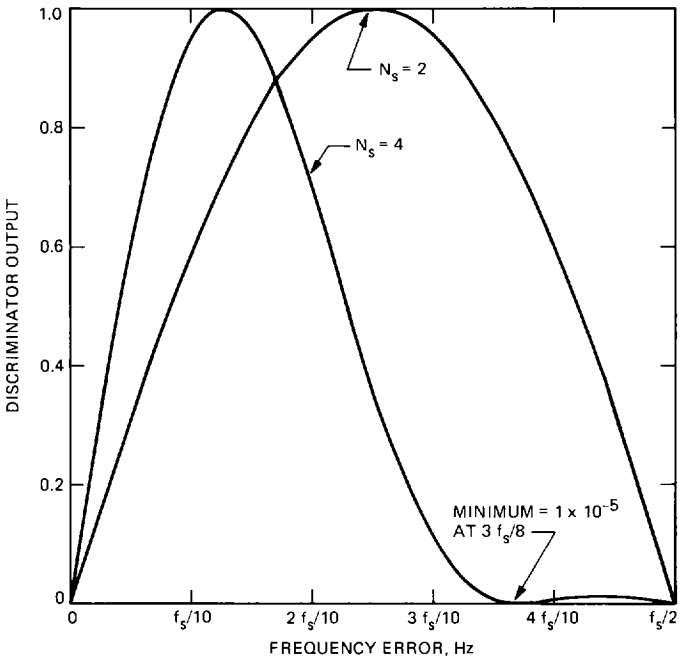

Fig. 3. Normalized discriminator curves for ODAFC loop (only positive frequency errors are shown)

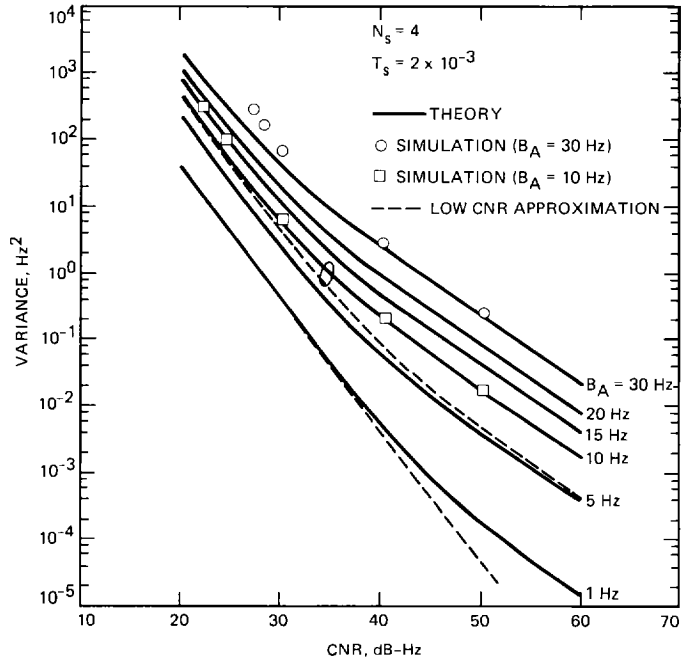

Fig. 4. Tracking performance of the ODAFC loop ($N_s = 4$) as a function of CNR with nominal bandwidth as a parameter

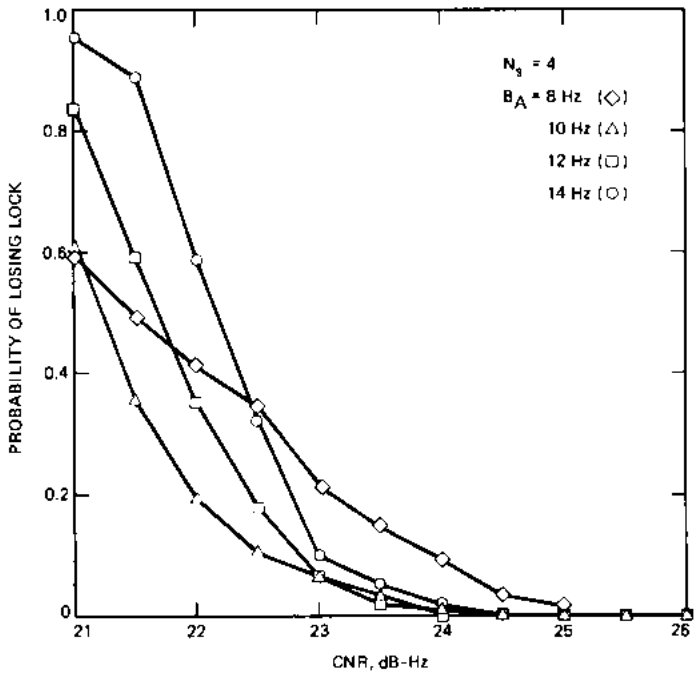

Fig. 5. Probability of losing frequency lock in a dynamic medium as a function of CNR with nominal bandwidth as a parameter (N_s = 4)

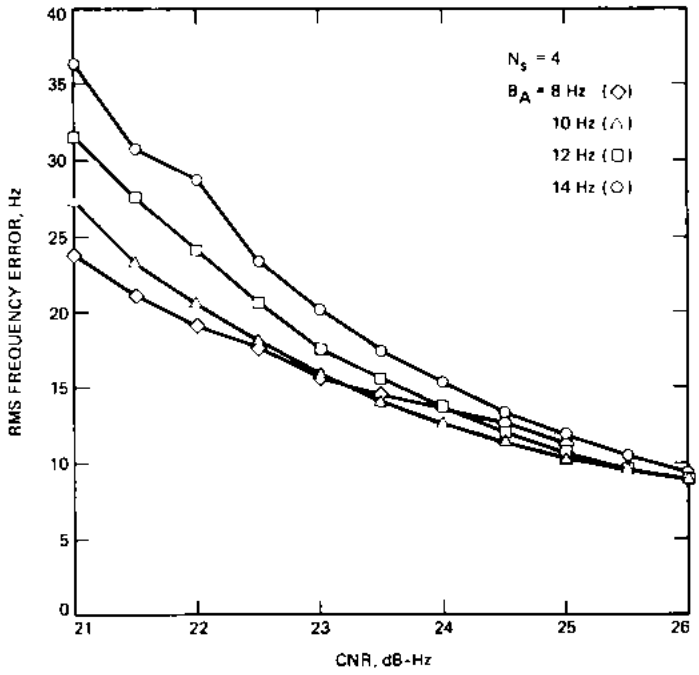

Fig. 7. Tracking performance of the ODAFC loop in a dynamic medium (N_s = 4)

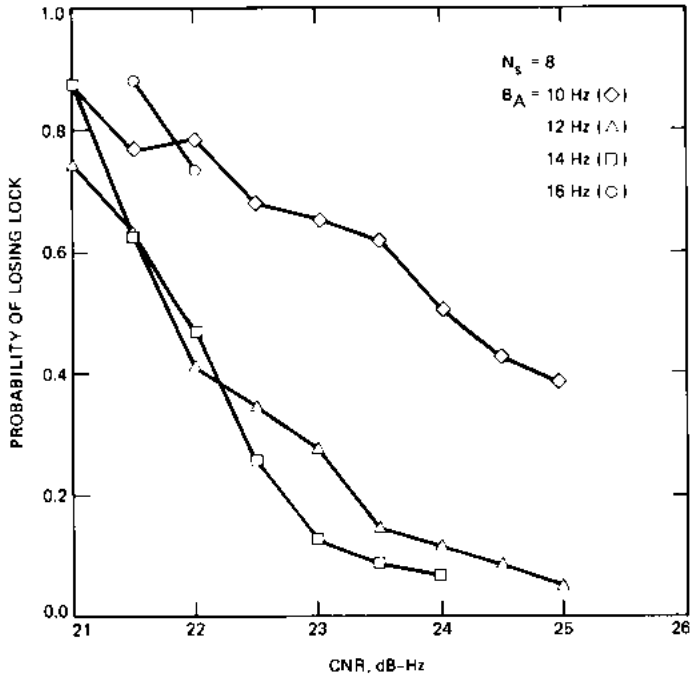

Fig. 6. Probability of losing frequency lock in a dynamic medium as a function of CNR with nominal bandwidth as a parameter (N_s = 8)

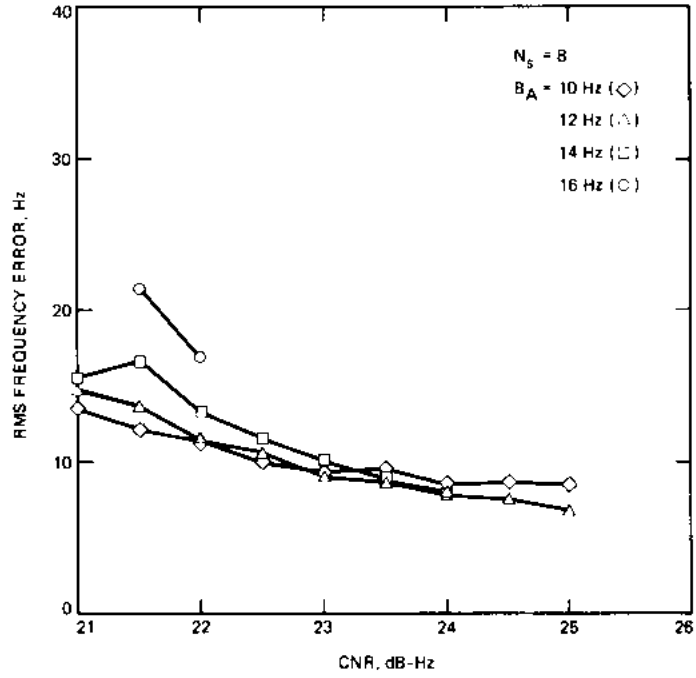

Fig. 8. Tracking performance of the ODAFC loop in a dynamic medium (N_s = 8)

Appendix A

Correlation Function of the Equivalent Additive Noise for the ODAFC Loop

In this appendix, the autocorrelation function of the equivalent additive noise for the ODAFC loop is computed for any lag. The starting point is Eq. (7). The autocorrelation is given by

$$R_{N_{eq}}(\ell) = \mathbb{E}\left(N_{eq,k}\, N_{eq,k+\ell}\right)$$

$$= 4\left(\frac{1}{N_s}\right)^4 \sum_{\substack{m=k \\ -(N_s-1)}}^{k} \sum_{\substack{n=k \\ -(N_s-1)}}^{k} \sum_{\substack{i=k+\ell \\ -(N_s-1)+\ell}}^{k+\ell} \sum_{\substack{j=k+\ell \\ -(N_s-1)+\ell}}^{k+\ell} \Big\{ A^2\sigma^2\delta_{mi} \times \cos(\phi_n - \phi_j) - A^2\sigma^2\delta_{mj}\cos(\phi_n - \phi_i)$$

$$- A^2\sigma^2\delta_{ni}\cos(\phi_m - \phi_j) + A^2\sigma^2\delta_{nj}\cos(\phi_m - \phi_i)$$

$$+ 2\sigma^4\delta_{nj}\delta_{mi} - 2\sigma^4\delta_{mj}\delta_{ni}\Big\} C_{mn}C_{ij} \qquad \text{(A-1)}$$

where

$$\delta_{xy} = \begin{cases} 1 & x = y \\ 0 & x \neq y \end{cases} \qquad \text{(A-2)}$$

$$C_{xy} = \sin\left(\frac{\pi}{N_s}(x-y)\right) \qquad \text{(A-3)}$$

For linear analysis it is useful to make the approximation $\cos(\phi_x - \phi_y) = 1$ in Eq. (A-1); therefore, the correlation function becomes

$$R_{N_{eq}}(\ell) \approx 4\left(\frac{1}{N_s}\right)^4 \sum_{m=0}^{N_s-1} \sum_{n=0}^{N_s-1} \sum_{i=\ell}^{N_s-1+\ell} \sum_{j=\ell}^{N_s-1+\ell} \Big\{ A^2\sigma^2\delta_{mi} - A^2\sigma^2\delta_{mj} - A^2\sigma^2\delta_{ni} + A^2\sigma^2\delta_{nj}$$

$$+ 2\sigma^4\delta_{mi}\delta_{nj} - 2\sigma^4\delta_{mj}\delta_{ni}\Big\} C_{mn}C_{ij} \qquad \text{(A-4)}$$

Due to symmetry, the previous correlation reduces to

$$R_{N_{eq}}(\ell) \approx 16\left(\frac{1}{N_s}\right)^4 A^2\sigma^2 \sum_{m=0}^{N_s-1} \sum_{n=0}^{N_s-1} \sum_{i=\ell}^{N_s-1+\ell} \sum_{j=\ell}^{N_s-1+\ell} \delta_{mi}\, C_{mn} \times C_{ij} + 16\left(\frac{1}{N_s}\right)^4 \sigma^4 \sum_{m=0}^{N_s-1} \sum_{n=0}^{N_s-1} \sum_{i=\ell}^{N_s-1+\ell} \sum_{j=\ell}^{N_s-1+\ell} \delta_{mi} \times \delta_{nj}\, C_{mn}\, C_{ij} \qquad \text{(A-5)}$$

or, using short notation:

$$R_{N_{eq}}(\ell) \approx C_1 f_{11} - C_1 f_{12} + C_2 f_{21} - C_2 f_{22} \qquad \text{(A-6)}$$

where

$$C_1 \triangleq 8\left(\frac{1}{N_s}\right)^4 A^2\sigma^2$$

$$C_2 \triangleq 8\left(\frac{1}{N_s}\right)^4 \sigma^4 \qquad \text{(A-7)}$$

and

$$\left.\begin{aligned} f_{11} &= \sum\sum\sum\sum \delta_{mi} \cos\left[\frac{\pi}{N_s}(m-n+j-i)\right] \\ f_{12} &= \sum\sum\sum\sum \delta_{mi} \cos\left[\frac{\pi}{N_s}(m-n+i-j)\right] \\ f_{21} &= \sum\sum\sum\sum \delta_{mi}\delta_{nj} \cos\left[\frac{\pi}{N_s}(m-n+j-i)\right] \\ f_{22} &= \sum\sum\sum\sum \delta_{mi}\delta_{nj} \cos\left[\frac{\pi}{N_s}(m-n+i-j)\right] \end{aligned}\right\} \qquad \text{(A-8)}$$

For simplicity, the limits in the summations have been omitted, but are equal to those of Eq. (A-3). After considerable algebra, the functions in Eq. (A-6) reduce to

$$f_{11} = \frac{(N_s - |\ell|)\cos\left[\frac{\pi}{N_s}\ell\right]}{\left[\sin\left(\frac{\pi}{2N_s}\right)\right]^2} \qquad 0 \leqslant |\ell| \leqslant N_s \qquad \text{(A-9)}$$

$$f_{12} = \frac{\sin\left(\frac{\pi|\ell|}{N_s}\right)}{\sin\left(\frac{\pi}{N_s}\right)}\left[\frac{1}{\sin\left(\frac{\pi}{2N_s}\right)}\right]^2 \qquad 0 \leqslant |\ell| \leqslant N_s \qquad \text{(A-10)}$$

$$f_{21} = (N_s - |\ell|)^2 \qquad 0 \leqslant |\ell| \leqslant N_s \qquad \text{(A-11)}$$

$$f_{22} = \left[\frac{\sin\left(\frac{\pi\ell}{N_s}\right)}{\sin\left(\frac{\pi}{N_s}\right)}\right]^2 \qquad 0 \leqslant |\ell| \leqslant N_s \qquad \text{(A-12)}$$

After collecting the terms in Eqs. (A-9)–(A-12) and using Eq. (A-6), the correlation function shown in the main text is obtained.